https://publications.dainst.org

iDAI.publications

DIGITALE PUBLIKATIONEN DES
DEUTSCHEN ARCHÄOLOGISCHEN INSTITUTS

Das ist eine digitale Ausgabe von / This is a digital edition of

Nami, Mustapha – Moser, Johannes

La grotte d'Ifri n'Ammar: t. 2 Le Paléolithique Moyen

der Reihe / of the series

Forschungen zur Archäologie außereuropäischer Kulturen; 9

DOI: https://doi.org/10.34780/o4kz-q423

Appendix C

Themoluminescence dating of heated flint artefacts from Ifri n'Ammar

Daniel Richter

Establishing a chronology for any given site is crucial to our understanding and reconstruction of past human activities and historical process. While relative chronostratigraphies can be established for Palaeolithic sites by means of techno-typological analysis of the lithics on basis of the relative stratigraphies, it is only by chronometric dating that these frameworks can be fixed on a timescale. However, proxy data often can provide more precise estimates of the time involved in the accumulation of the sediments and cultural remains. But such approaches often lack accuracy, as they provide only relative age information, unless fix points can be defined. While the stratigraphy serves as a basic tool for establishing the age of a sequence, chronometric dating can provide such fix points. One of such methods is thermoluminescence (TL) dating of heated flint artefacts. The event dated is the last heating of rock material, and thus the time elapsed since the prehistoric human activity of lighting a fire is determined. It is one of the few instances where chronometric dating can provide an age estimate of a prehistoric activity directly (Richter 2007). Natural fires in caves are rare (see discussion in Alperson-Afil *et al.*, 2007) and heat penetration of natural fire into sediment is low (Bellomo, 1993). Therefore any rock material which is covered by a few centimetres of sediment only is not heated to an extent that would allow TL dating and thus the association of the sample and the event dated is secure. Heated flint artefact samples from the two layers of the 'occupation supérieure' ('Upper OS' and 'Lower OS') as well as from the 'occupation inférieure' ('Upper OI and 'Lower OI') were available for TL dating analysis.

METHOD OF THERMOLUMINESCENCE (TL) DATING

Thermoluminescence (TL) dating of heated flint artefacts is based on the accumulation of metastable charges (palaeodose) in the crystal lattice by ionizing radiation since the last heating of the rock (Aitken, 1985). Such structural damages in the crystal lattice of minerals are caused by the decay of radioactive elements from the surrounding sediment (external dose) and the sample itself (internal dose), as well as secondary cosmic rays (external dose). This omnipresent ionization causes a radiation dose (palaeodose or P) to accumulate in the crystal in the form of electrons in excited states. For dating application only electrons in metastable states are targeted, which are resident over periods of time much longer then the anticipated age (approximately 50 Ma, Wintle and Aitken, 1977). Detailed descriptions of the principles of luminescence dating methods can be found elsewhere (Aitken, 1985; Aitken, 1998; Wagner, 1998; Bøtter-Jensen *et al.*, 2003), and a general account of TL dating of lithics is given in Richter (2007).

The palaeodose (P) is a function of the dose rate ($\dot{D}$; the ionizing radiation per time unit), which provides the clock for the dating application and the time scale the crystal was exposed to the omnipresent radiation. Exposure to light or elevated temperatures causes the electrons to relax to a ground state, sometimes by emitting a photon, which is the luminescence. If the temperature is high enough ($> \sim 400° \text{C}$) the drainage is sufficient to relax all electrons relevant to the luminescence method used, i. e. the clock is set to zero by this event. After cooling the radiation dose starts to accumulate again and as a consequence the intensity of the luminescence signal (number of photons) increases with the total absorbed dose (P) in a crystal and is therefore a function of exposure time to radiation.

The age is obtained by the ratio of the palaeodose to the sum of a series of dose-rates under the assumption of the constancy of the ionizing radiation (dose-rate) over the entire burial time (Aitken 1985):

$$\text{age}_{(ka)} = \frac{P_{(Gy)}}{\dot{D}_{(Gy \cdot a^{-1})}} = \frac{P}{\dot{D}_{(internal)} + \dot{D}_{(external)}} = \frac{P}{(\eta\dot{D}_\alpha + \dot{D}_\beta + \dot{D}_\gamma) + (\dot{D}_\gamma + \dot{D}_{cosmic})} = \frac{P}{(\eta\dot{D}_{\alpha(U)} + \eta\dot{D}_{\alpha(Th)} + \dot{D}_{\beta(U)} + \dot{D}_{\beta(Th)} + \dot{D}_{\beta(K)} + \dot{D}_{\gamma(U)} + \dot{D}_{\gamma(Th)}) + (\dot{D}_\gamma + \dot{D}_{cosmic})}$$

where the palaeodose (P) is expressed in Gy and the dose rates in Gy per time unit (usually in a or ka).

The denominator $\dot{D}$ of the age formula consists of two sets of parameters, the internal ($\dot{D}_{internal}$) and the external dose rates ($\dot{D}_{external}$). Any variability of one of the parameters of $\dot{D}$ through time makes it difficult to estimate the age of a heated flint (e. g. Richter, 2007). All parts of the samples which are considered to be potentially geochemical instable, like cortex or patinated portions are carefully removed with a water cooled diamond saw from the flint samples prior to TL-dating. The internal dose-rate ($\dot{D}_{internal}$), which is measured on a subset of the sample by Neutron Activation Analysis (NAA), is thus considered as being constant over the time-span of interest. This is an advantage of heated flint TL-dating over most other dosimetric dating methods, and reduces the uncertainty given for any age estimate. Most uncertainties in TL-dating of heated flint derive from the estimates of uncertainties associated with the ionizing radiation from the surrounding sediment ($\dot{D}_{external}$) which is measured by either gamma spectrometry or insertion of dosemeters in the sediments for a specified period of time. In order to simplify the estimation of $\dot{D}_{external}$, and thus reduce the overall uncertainty of an age estimate, each sample is carefully stripped of its outer 2 mm surface area (approximately the range of β-radiation from isotopes contained in the surrounding sediment).

Measurement parameters and sample preparation

Because the luminescence signal of most of the samples from Ifri n'Ammar is at the onset of saturation, the palaeodose on the 90-160 µm fractions of the crushed flint material (after the removal of the outer 2 mm with a water cooled low speed saw) was obtained by a multi-aliquot-additive-regeneration (MAAR) slide protocol (Figure 1). A comparison of the data sets which could be analysed using a standard linear approximation approach (e.g. Richter *et al.* 2000) revealed no significant differences in results, already at the confidence level of 68 %. In fact, individual as well as averaged results are virtually identical. Therefore a single analytical procedure which is appropriate for all samples was used. The alpha contribution to the natural and additive TL-signals is subtracted and the TL data is described by quadratic functions and shifted along the dose axis (Valladas and Gillot 1978; Mercier 1991) after scaling of the regeneration curve (Sanzelle *et al.* 1996). This procedure is similar to the Australian Slide Method (Prescott *et al.* 1993). An iteration procedure then corrects for the underestimation of the alpha contribution for samples at the onset of saturation, which is based on a linear approximation (Mercier 1991). Between 6 and 12 aliquots were used for each of the 4-5 dose points for each of the two growth curves, where the grains for the regeneration growth curve were heated to 360°C for 90 min in air before irradiation. This procedure is assumed to induce the least sensitivity changes. Carbonates were removed with acetic acid after crushing and/or heating. Thermoluminescence was detected with an 'EMI 9236QA' photomultiplier with detection restricted to the UV-blue wavelength band by Schott BG25 and WG5 filters at a heating rate of 5°C min⁻¹ to 450°C on Risø DA-20 or DA-15 systems. Irradiations were performed with external calibrated sources (β with $^{90}Y/^{90}S$ at ~0.26 Gy s⁻¹ and α with ^{214}Am at 0.178 µm min⁻¹). The alpha sensitivity (b-value after Bowman and Huntley 1984) was determined by an additive approach for the samples from layers 'Upper OS' and 'Lower OS' and by comparing the luminescence response of 4-11 µm fine grain material which was heated in air to 500°C for 30 min of single doses from alpha and beta irradiation for layers 'Upper OI' and 'Lower OI'. A comparison test revealed no differences in these approaches for other samples, which is assumed to be the case here as well. The integration range of the luminescence signal was defined by the range of overlap of the temperature ranges of the heating plateau (Figure 2) with the equivalent dose plateau in order to achieve the most accurate and precise results.

Fig. 1. TL growth curves of sample EVA-LUM-07/05 showing the additive growth curve in blue, the regenerated growth curve in red and the shifted regeneration growth curve in green.
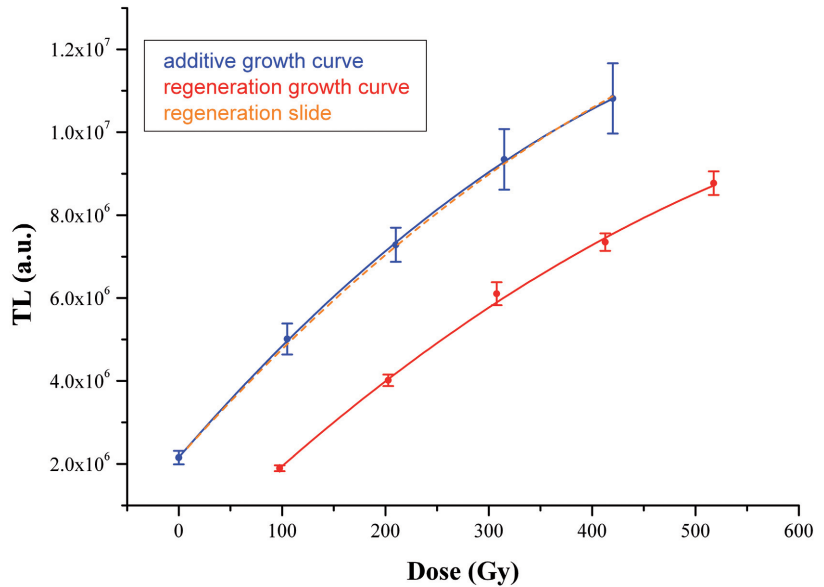
Fig. 2. TL glow curves and heating plateau of sample EVA-LUM-05/03. The natural TL-signals (NTL) is shown in blue, the additive TL-signals (NTL+β) in red and the ratio of NTL+β to NTL over temperature (heating plateau defined as the temperature range of constant ratio) in grey.
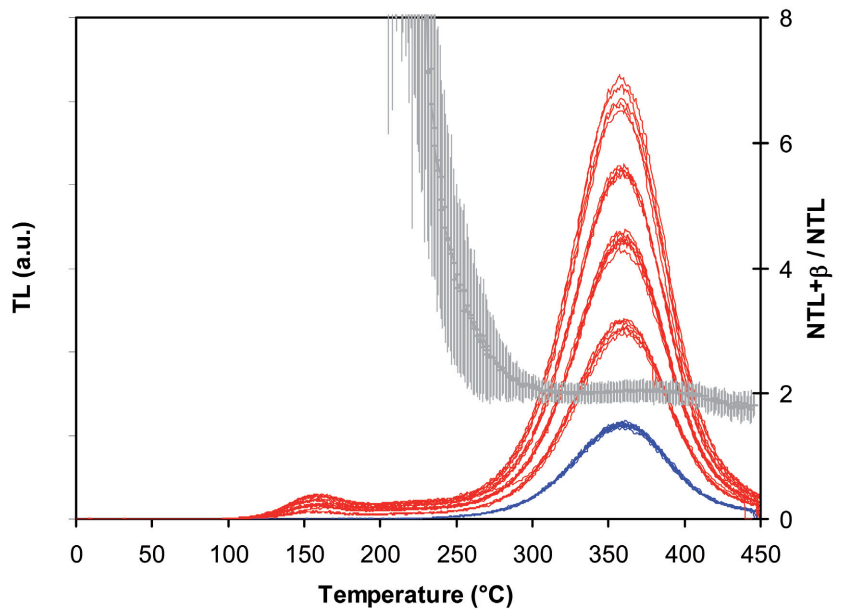
SAMPLE SELECTION, TESTING AND REJECTION

A small portion from the outer edge of each heated flint submitted for dating was analysed in order to determine the correct attribution of heat alteration for each individual sample. The physical evidence for a raised temperature is achieved by analysing the TL response from the natural sample (unirradiated natural) in relation to the TL signal from a portion which has received an additional dose (natural + dose) from a calibrated radioactive β-source. The flat ratio (plateau) of the 2 signals over temperature indicates the presence of the pre-historic zeroing of the TL-signal for a given temperature. In cases of no prehistoric heating or where the heating was less to about 400°C the ratio of the 2 signals is not uniform at all or might be flat for a short temperature range only, respectively. In such cases the lack of a plateau in the range of the peak temperatures indicates the insufficiency of the heating for dating analysis. An additional criterion of prehistoric heating is the presence of a single peak with a shape similar to a Gaussian distribution (Figure 2), lacking shoulders at either side and the peak temperature occurring in a range between 350 and 380°C. Only

such samples were considered. If the flat ratio extends over the TL peak temperature, a 'heating plateau' (Aitken, 1985) is defined and the sample is confirmed to have been sufficiently heated for TL analysis (Figure 2). Such samples were then prepared for full TL analysis (see sample preparation) and the test was repeated with this extracted material in order to verify that the temperatures achieved in the interior of the sample were sufficient to fully erase the TL-signal and full fill a fundamental assumption in TL-dating of heated flint artefacts. Only such samples were subsequently used for dating analysis.

A total of 60 artefacts showing macroscopic traces of heating, like potlids, craquelation, reddening (Richter, 2007), were submitted for TL-analysis. In six cases the macroscopic analysis could not be confirmed with thermoluminescence. Another seven samples showed signs of only moderate heating and were thus rejected from analysis. For four samples the TL-signal could not be artificially regenerated to a shape and temperature similar to the observed natural TL-signal. They were therefore rejected as well, as they would have provided only minimum age results because the correction of the supralinearity would not be considered to be reliable. While analysis would have been possible for another four samples only with appropriate preheating conditions, they were not used either because of the abundance of samples for this site and the potential difficulties associated with the necessary preheating for isolating the peak used for dating. Two samples were found to be too close to TL-signal saturation for analysis. Another two samples did not yield enough sample material for standard analysis and the application of a special short SAR protocol (Richter & Krbetschek, 2006) will be applied in the near future. TL-age results are therefore provided for a total of 35 samples, with 10 from layer 'Upper OS', 9 from 'Lower OS' (Tables 4–5) published in Richter *et al.* (in press), 9 from 'Upper OI' and 7 from 'Lower OI' (Tables 6–7) published in Richter *et al.* (submitted_a).

Dosimetry

The internal dose rates ($\dot{D}_{internal}$) were calculated after Adamiec and Aitken (1998) based on Neutron Activation Analysis results for U, Th and K on 200 mg of sample material less than 160 μm from the extracted cores, which were obtained prior the chemical treatment.

Dosimetric dating methods are based on the assumption of the stability of the dose rates over the burial time and the homogeneous distribution of radioactive elements in the sample. However, either can be modelled as well (e.g. Guibert *et al.* 2009; Tribolo *et al.* 2006). The flint samples here do not exhibit a large variability of grain sizes on the microscopic scale and inhomogeneities are therefore unlikely. The stability of the internal dose rates can not be contested over the time range of interest because only those parts of the samples were used for analysis, which did not show any macroscopical traces of geochemical alterations, like patination.

The stability of the external γ-dose rate from the surrounding sediment was verified by HpGe γ-ray spectrometry based on a SiO_2 matrix of sediment samples from each layer, which do not exhibit disequilibria of neither the U nor the Th decay chain (Table 1). While these analyses do not reject the possibility of very ancient occurrences of disequilibria we interpret the lack of such and the absence of any trends in ratios of analysed isotopes through the sediment column as indications that the decay chains have always been in secular equilibrium. The external γ-dose rate is thus assumed to have been stable over the entire burial period.

HpGe γ-ray spectrometry does allow the analysis of the small particles of the sediments only. But the sediment layers at Ifri n'Ammar contain larger pieces of rocks. HpGe γ-ray spectrometry on sediment samples in the laboratory is therefore not representative because the site's dosimetry has to be considered as 'lumpy' (after Schwarcz 1994). The external γ-dose was therefore measured with α-Al_2O_3:C dosemeters which were buried 30 cm deep into the profiles for the duration of one year at a spacing of about 60 cm for each layer in all the exposed profiles available (Table 2). They record the true γ-dose rate at their individual positions and exhibit a large variation (Table 2) with differences of up to a factor of almost two. This is an indication of the 'lumpiness' of the site. The positions occupied by the dosemeters are assumed to be similar to the ones occupied by the flint samples, which are originating from different positions within a given layer. The γ-dose rates are obtained by comparing each crystals OSL response (5 crystals in each dosemeter) of the natural one

sediment sample	238U serie						232Th serie				K	
	238U (A/m / Bq/kg)	±	226Ra (A/m / Bq/kg)	±	210Pb (A/m / Bq/kg)	±	228Ra (A/m / Bq/kg)	±	228Th (A/m / Bq/kg)	±	40K (A/m / Bq/kg)	±
Upper OS	10.15	1.04	11.58	0.36	9.57	1.00	10.50	0.70	10.33	0.54	325.94	1.81
Lower OS	10.54	0.64	11.29	0.31	9.96	0.76	10.36	0.61	10.01	0.49	328.75	1.44
Upper OI	12.39	1.27	13.60	0.46	14.37	1.60	15.92	1.07	14.76	0.79	411.65	2.50
Lower OI	10.75	1.23	11.16	0.37	11.49	1.29	10.46	0.75	9.97	0.55	368.79	2.17

Tab. 1. Results from HpGe γ-ray spectrometry on dry sediment samples. For ^{238}U the γ-lines from ^{234}Th, ^{234m}Pa, ^{235}U; for ^{226}Ra from ^{214}Pb, ^{214}Bi and for ^{228}Ra from ^{228}Ac; for ^{228}Th from ^{212}Pb, ^{212}Bi, ^{208}Tl were used.

Dosemeter #	square	x	y	z (datum)	$\dot{D}_{\gamma\text{-ext.}}$ (µGy a-1)
V-1	H17	30	80	6.90	359
V-2	I17	30	66	6.90	555
V-3	I17	30	26	6.95	421
V-4	I17	30	67	6.85	426
average					440
VII-1	L17	64	70	5.54	455
VII-2	L13	55	70	5.69	733
VII-3	L12	95	70	5.60	490
average					559
XII-1	L15	64	70	4.73	755
XII-2	L14	81	70	4.73	624
XII-3	L14	6	70	4.73	588
XII-4	L13	41	70	4.78	643
XII-5	L12	8	70	4.83	659
average					654
XXI-1	L12	62	70	3.95	569
XXI-2	L14	98	70	3.98	543
XXI-3	L14	35	70	4.00	failed
XXI-4	L13	70	70	3.96	311
XXI-5	L13	23	70	3.96	574
average					499

Tab. 2. Positions and γ-dose rates ($\dot{D}_{\gamma\text{external}}$) of α-Al$_2O_3$:C dosemeters. Values are for present day moisture except for 'Upper OS', which were corrected as described in the text. For age calculation additional moisture of 10 and 20% for prehistoric conditions of layers 'Upper OI' and 'Lower OI', respectively, was assumed, which results in average external γ-dose rates of 591 and 411 µGy a^{-1} respectively.

layer	dry $\dot{D}_{\gamma\text{-ext.}}$ (µGy a-1)	natural moisture (%)	wet $\dot{D}_{\gamma\text{-ext.}}$ (µGy a-1)	water saturation (%)	saturated $\dot{D}_{\gamma\text{-ext.}}$ (µGy a-1)	saturated/wet γ-dose rate
Upper OS	474	20	391	53	303	0.77
Lower OS	475	6	446	28	366	0.82
Upper OI	626	10	567	34	460	0.81
Lower OI	511	12	454	40	258	0.57

Tab. 3. Natural moisture (%) from sealed sediment samples from each layer and water saturation (%) with the corresponding γ-dose rates (µGy a⁻¹) as obtained by HpGe γ-ray spectrometry on dry sediment samples. Adjusted values for the latter providing γ-dose rates for the natural moisture as well as for water saturation. The reduction of the γ-dose rates for saturated environments is given as the ratio of saturated/wet γ-dose rates.

year exposure to an artificial irradiation by a Cs-source. The high accuracy and precision of this approach has been recently shown by comparison with HpGe γ-ray spectrometry (Richter *et al.*, submitted_b). Analytical uncertainties of dosemeter measurements are typically between 2 and 5 %, but for age calculation an uncertainty of 20 %, which is equivalent to the average variability of the γ-dose rate as observed by the dosemeters, was used for the external γ-dose rate.

For layer 'Upper OS' four dosemeters were placed at the only available profile at the mouth of the cave which resulted in a maximum distance to the samples of 5 m. For the other layers the main NE-profile was available for dosimetry and for the majority of samples the distances were smaller than the maximum of 3 m. Three dosemeters could be placed in layer 'Lower OS', and 5 each in layers 'Upper OI' and 'Lower OI', where for the latter one dosemeter failed the quality criteria for reading out the dose (Table 2). The moisture content of the sediments was determined in the laboratory on sealed samples (Table 3) and differences by a factor of two were observed between samples originating from the inside of the cave (6-10 %) and at the drip line area (20 %). The γ-dose rates for the dosemeters in layer 'Upper OS' were therefore adjusted accordingly to a reduced moisture value of 10 %, because the samples dated are all coming from inside the cave and were not influenced by water from the drip line which, in addition, was located further north in the past. Otherwise the age results for layer 'Upper OS' would be overestimated because of the reduced γ-dose rate due to the influence of dripping water in the area of the present day

measurement positions. No attempts were made to estimate an average moisture value for the entire burial time of the samples from layer 'Upper OS' and 'Lower OS'. However, caliche deposits between and above the layers 'Upper OI' and 'Lower OI' indicate the presence of large amounts of water. Especially the lowest level must have been saturated with water at times because it is located very close to the bedrock and a standing water table is probably necessary for the formation of these caliches. But this situation was episodical and it is not possible to estimate the time required for the formation of the caliche deposits observed and to calculate an average moisture as is required for TL age calculation. The present day moisture values are certainly too low because today the wadis are lower in elevation compared to the past and sediments therefore are certainly drier today. Therefore it is likely that there were times of water saturation at least of the lowest layer which has to be accounted for. As a conservative approach, an additional 10 and 20 % increased moisture for the sediments of layers 'Upper OI' and 'Lower OI', respectively, is assumed in order to correct for the reduced γ-dose rate (Table 2) in prehistoric times. These values are believed to represent minimum estimates only and therefore the resulting TL ages have to be considered as minimum age estimates. However, the influence of the sediment moisture on the γ-dose rate is not very large (e.g. a change in 10 % moisture results in a change of approximately 10 ka, which is within uncertainties). The assumed uncertainty of 20 % for the external γ-dose rate also incorporates possible large fluctuations resulting from varying moisture levels and is identical to the average relative standard

EVA-LUM	Palaeodose (Gy)	b-value (Gy μm²)	U (ppm)	Th (ppm)	K (ppm)	$\dot{D}_{int.eff}$ (μGy a⁻¹)	$\dot{D}_{-\gamma\text{-}ext.eff.}$ (μGy a⁻¹)	$\dot{D}_{cosmic}$ (μGy a⁻¹)	$\dot{D}_{internal}$ (% $\dot{D}_{total}$)	Age (ka)
05/01	75.9 ± 0.6	1.16 ± 0.03	0.99 ± 0.07	0.02 ± 0.01	497 ± 124	203 ± 14	409	52	31	114.2 ± 17.8
05/02	45.9 ± 0.2	1.90 ± 0.02	0.62 ± 0.06	0.08 ± 0.05	1,530 ± 199	233 ± 18	416	52	33	65.5 ± 6.1
05/03	109.9 ± 7.8	1.12 ± 0.01	2.08 ± 0.10	0.06 ± 0.02	291 ± 157	368 ± 19	418	52	44	131.2 ± 18.3
05/04	52.8 ± 0.5	2.07 ± 0.01	0.66 ± 0.06	0.19 ± 0.03	998 ± 210	204 ± 18	400	52	31	80.3 ± 12.4
05/05	69.0 ± 1.3	1.86 ± 0.03	0.87 ± 0.08	0.24 ± 0.04	1,010 ± 323	242 ± 28	414	52	34	97.5 ± 14.7
05/06	53.3 ± 1.4	2.45 ± 0.02	0.60 ± 0.07	0.12 ± 0.03	1,200 ± 312	228 ± 26	403	52	33	78.2 ± 11.8
05/07	62.3 ± 0.1	1.33 ± 0.02	0.90 ± 0.08	0.18 ± 0.04	1,490 ± 298	274 ± 26	418	52	37	83.7 ± 12.4
05/08	53.9 ± 2.0	1.52 ± 0.01	0.46 ± 0.06	0.11 ± 0.04	1,280 ± 294	183 ± 25	418	52	28	82.5 ± 13.2
05/12	55.3 ± 1.4	1.50 ± 0.02	0.51 ± 0.06	0.40 ± 0.08	1,260 ± 34	200 ± 9	420	52	30	82.3 ± 13.0
06/18	71.2 ± 3.9	1.22 ± 0.03	0.68 ± 0.08	0.22 ± 0.04	1,420 ± 38	231 ± 12	425	52	33	100.6 ± 15.5
							weighted average			83 ± 6

Tab. 4. Layer 'Upper OS'. Results of TL measurements, Neutron Activation Analysis, dosimetry and ages. Uncertainties used in age calculation for $\dot{D}_{-\gamma\text{-}ext.eff.}$ and $\dot{D}_{cosmic}$ are 20 and 5 % respectively (see text). The external γ-dose rate was adjusted for decreased moisture of 10 % because the present day measurements were done in an area much wetter than the sample positions.

deviations (RSD) of γ-dose rates obtained by the α-Al$_2$O$_3$:C dosemeters.

The cosmic dose was estimated by taking into account the thickness and shape of the cave and the thickness of the sediments (Prescott & Hutton, 1994; Prescott & Stephan, 1982), employing a 5 % uncertainty after Barbouti and Rastin (1983).

Thermoluminescence dating results

Thermoluminescence dating of heated flint from Palaeolithic sites is often hampered by the inhomogeneous nature of the sediment with variable contents of larger rock material, which results in a 'lumpy' dosimetric environment. Therefore each sample is exposed within a different geometry for external γ-radiation, which depends on the sediment composition of a sphere of approximately 60 cm diameter around the sample. Such individual positions/geometries can not be reproduced by any dose measurements and only reconstructed by modelling. However, the samples are removed from context during excavation and in most cases it is not feasible to document an excavation to the precision required for an accurate reconstruction of the dosimetric environment of each individual sample. As a consequence, the exact geometry for any sample can not be determined and has to be considered as

unknown. The inhomogeneities are at a scale of several centimetres and the use of the nearest dosemeter would therefore not solve the problem. The only way to approach this problem is by using an average value for the external γ-dose by measuring the dosimetric environment with a large number of dosemeters, which are placed in random positions in the sediment profiles in unknown geometries. Obviously this value is likely not the right one for any of the samples for dating and as a consequence none of the sample ages is calculated with the true external γ-dose rate. The use of values different than the correct one leads to an increased spread of ages. However, samples are selected for their property of being burnt, and not for their position in the sediment, and positions of dosemeters are not known *a priori* either as they are placed 30 cm deep in profiles at random geometries as well. But taken together, the averages of dosemeter values as well as sample doses will provide a good approximation of the true age if either number is large. Obviously a basic assumption is that the burning of all samples from one layer has to have taken place at roughly the same time or at least within uncertainties of the method (Richter, 2007).

The ranges of age estimates (Tables 4–7) obtained for the layers of Ifri n'Ammar are very large (Richter *et al.* in press; submitted_a). The relative standard deviations (RSD) of age

EVA-LUM	Palaeodose (Gy)	b-value (Gy μm²)	U (ppm)	Th (ppm)	K (ppm)	$\dot{D}_{int.eff}$ (μGy a⁻¹)	$\dot{D}_{-\gamma\text{-}ext.eff.}$ (μGy a⁻¹)	$\dot{D}_{cosmic}$ (μGy a⁻¹)	$\dot{D}_{internal}$ (% $\dot{D}_{total}$)	Age (ka)
05/09	127.6 ± 2.5	1.26 ± 0.02	1.26 ± 0.11	0.26 ± 0.06	1,930 ± 560	370 ± 47	531	47	39	134.6 ± 20.0
06/14	107.2 ± 3.8	1.29 ± 0.01	0.57 ± 0.04	0.07 ± 0.02	840 ± 235	164 ± 19	539	47	22	142.9 ± 24.7
05/10	98.4 ± 4.3	1.62 ± 0.02	0.60 ± 0.06	0.07 ± 0.03	366 ± 77	135 ± 10	520	47	19	140.2 ± 24.7
05/11	75.7 ± 0.6	1.22 ± 0.02	0.60 ± 0.05	0.06 ± 0.03	590 ± 159	148 ± 15	525	47	21	105.0 ± 18.2
06/15	135.5 ± 2.5	1.93 ± 0.02	1.03 ± 0.06	0.11 ± 0.03	1,770 ± 336	326 ± 28	531	47	36	149.9 ± 22.8
07/04	135.3 ± 1.8	1.53 ± 0.02	1.20 ± 0.09	0.09 ± 0.04	505 ± 17	249 ± 13	531	47	30	163.7 ± 26.2
07/05	90.5 ± 0.9	1.05 ± 0.03	0.43 ± 0.06	0.09 ± 0.03	308 ± 11	97 ± 9	542	47	14	131.9 ± 24.1
06/16	97.0 ± 3.9	0.96 ± 0.03	1.08 ± 0.07	0.18 ± 0.03	1,750 ± 298	318 ± 25	514	47	36	110.3 ± 16.9
06/17	90.1 ± 3.4	0.97 ± 0.02	0.53 ± 0.04	0.13 ± 0.03	371 ± 12	119 ± 6	534	47	17	128.7 ± 23.1
								weighted average		130 ± 8

Tab. 5. Layer 'Lower OS'. Results of TL measurements, Neutron Activation Analysis, dosimetry and ages. Uncertainties used in age calculation $\dot{D}_{-\gamma\text{-}ext.eff.}$ and $\dot{D}_{cosmic}$ are 20 and 5 % respectively (see text).

results are similar to those for the dosemeter readings. In fact RSDs of both follow the same pattern through the stratigraphy which is indicating that the observed variability of external γ-dose rates is directly reflected in the age results (see above). The relative average deviations from the means as a measure of the variability of the data are in the range (except for 'Lower OI') of the uncertainty of 20 % which was assumed for the external γ-dose rate. After rejection of statistically significant outliers the RSDs are obviously much smaller than the above uncertainty, which can be taken as an indication that the assumed uncertainty is including factors of variability which are affecting the age.

Ten heated flint samples were dated by TL from layer 'Upper OS' (Table 4), resulting in a range between 65 to 131 ka (Richter *et al.* in press). No outlier was detected with a Dixons test (after Rorabacher 1991) and a Shapiro-Wilk test (software Origin 8) shows that the data is a sample from normally distributed data. A weighted mean of 83 ± 6 ka was calculated. The systematic uncertainties are included twice in all weighted mean calculations here, following Sachs (1992), in order to compensate for large sample numbers, which would eventually result in unrealistically small uncertainties of weighted means.

Eight heated flint samples were dated by TL from layer 'Lower OS' (Table 5), resulting in a range between 105 to 164 ka (Richter *et al.* in press). No outlier was detected with a Dixons test (after Rorabacher 1991) and a Shapiro-Wilk test (software Origin 8) shows that the data is

a sample from normally distributed data. The weighted mean for this data is 130 ± 8 ka.

Nine heated flint samples were dated by TL from layer 'Upper OI' (Table 6), resulting in an age range of 118 to 250 ka (Richter *et al.* to be written). Sample EVA-LUM-07/10 was detected as a significant outlier with a Dixons test (after Rorabacher 1991), which reduces the range of means to 118 to 161 ka. A Shapiro-Wilk test (software Origin 8) shows that this reduced data is a sample from normally distributed data. The weighted mean for this data is therefore 145 ± 9 ka after rejection of sample EVA-LUM-07/10.

Concerns can be raised about the influence of the assumed increased average moisture used to adjust the external γ-dose rate. While the values used appear to be the most appropriate and most conservative values, results from calculations of other scenarios are given in order to place the influence of this parameter and the preferred results in context, and allow for a better evaluation of the data presented here. Not adjusting for the past increased moisture content of the sediments, a fact which is evidenced by the caliche deposits, allows the calculation of a minimum age estimate for the samples resulting in a weighted average of 135 ± 9 ka. Employing the ratio of the measured wet to saturation moisture of the sediment in order to estimate the maximum possible water content for the entire burial time (which is an impossible scenario but provides a maximum age), the resulting weighted average age for the samples from layer 'Upper OI' is 155 ± 10 ka, which has to be considered as a maximum age

EVA-LUM	Palaeodose (Gy)	b-value (Gy µm²)	U (ppm)	Th (ppm)	K (ppm)	$\dot{D}_{int.eff}$ (µGy a⁻¹)	$\dot{D}_{-\gamma-ext.eff.}$ (µGy a⁻¹)	$\dot{D}_{cosmic}$ (µGy a⁻¹)	$\dot{D}_{internal}$ (% $\dot{D}_{total}$)	Age (ka)
05/13	118.2 ± 1.4	1.87 ± 0.02	0.36 ± 0.05	0.12 ± 0.03	1180 ± 189	160 ± 16	571	43	21	152.5 ± 26.8
07/09	157.0 ± 2.9	2.39 ± 0.01	1.60 ± 0.14	0.19 ± 0.05	1580 ± 43	429 ± 21	573	43	41	149.7 ± 21.9
06/22	123.6 ± 9.0	2.12 ± 0.01	0.81 ± 0.07	0.17 ± 0.05	1300 ± 221	255 ± 20	562	43	30	143.5 ± 23.6
06/23	122.8 ± 9.1	2.58 ± 0.01	0.77 ± 0.06	0.14 ± 0.03	1460 ± 248	265 ± 22	556	43	31	141.8 ± 23.0
07/10	344.6 ± 0.7	0.88 ± 0.01	4.72 ± 0.13	0.03 ± 0.01	184 ± 8	774 ± 19	562	43	56	249.5 ± 28.3*
07/11	120.1 ± 6.8	1.04 ± 0.01	0.59 ± 0.07	0.07 ± 0.03	579 ± 19	144 ± 10	570	43	19	158.4 ± 28.4
07/12	113.8 ± 8.7	1.31 ± 0.01	0.64 ± 0.05	0.10 ± 0.02	253 ± 11	131 ± 7	572	43	18	152.4 ± 27.8
05/14	141.9 ± 3.9	2.44 ± 0.04	1.06 ± 0.07	0.25 ± 0.04	693 ± 23	262 ± 10	573	43	30	161.0 ± 26.1
06/27	107.8 ± 1.3	0.9 ± 0.01	0.85 ± 0.15	0.25 ± 0.05	1890 ± 51	293 ± 23	573	43	32	118.5 ± 18.9
								weighted average$		145 ± 9

Tab. 6. Layer 'Upper OI'. Results of TL measurements, Neutron Activation Analysis, dosimetry and ages. Uncertainties used in age calculation $\dot{D}_{-\gamma-ext.eff.}$ and $\dot{D}_{cosmic}$ are 20 and 5 % respectively (see text). The external γ-dose rate was adjusted for 10 % increased moisture [* sample rejected by Dixon's outlier test; $ without rejected sample].

estimate. These data are statistically identical with each other, as well as with the preferred estimate of 145 ± 9 ka, which best represents the age of the last heating of the samples from this layer.

Seven heated flint samples were dated by TL from layer 'Lower OI' (Table 7), resulting in an age range from 147 to 340 ka (Richter *et al.*, submitted_a). Sample EVA-LUM-07/13 was detected as a significant outlier with a Dixons test (after Rorabacher 1991), which reduces the range of means to 147 to 199 ka. A Shapiro-Wilk test (software Origin 8) shows that this reduced data is a sample from normally distributed data. The weighted mean for this data is therefore 171 ± 12 ka after rejection of sample EVA-LUM-07/13.

The influence of the assumed average moisture used to adjust the external γ-dose rate are even more significant for this layer, because it forms the base of the sequence just above bedrock and during formation times of the caliche it is very likely that the sediment was water saturated for certain periods of time. Therefore a larger moisture correction was applied for samples from this layer. However, 20 % is still considered to be a conservative estimate. Results from calculations of other scenarios are given in order to place the influence of this parameter and the preferred results in context, and allow for a better evaluation of the data presented here. Omitting the adjustment for the past increased moisture of the sediments provides a minimum age estimate for the samples with a weighted average of 151 ± 12 ka. Adjusting for water saturation

for the entire burial time as described above (which is an impossible scenario) provides a maximum weighted average age for the samples from layer 'Lower OI' of 211 ± 15 ka. While the minimum and maximum estimates do not overlap statistically, both are in agreement with the preferred estimate of 171 ± 12 ka, which best represents the age of the last heating of the samples from this layer.

These four TL-data sets provide age ranges for the industries from the according levels. Statistically the three lower levels are of identical age with their upper and lower neighbour because the age ranges overlap at a significance level of 95 % (2σ). It is only the uppermost level 'Upper OS' being significantly younger, which is confirmed by a two sample T-test showing the two population means for level 'Upper OS' and 'Lower OS' to be significantly different, as is the case for 'Lower OS' and 'Lower OI'.

DATA COMPARISON WITH RADIOCARBON DATING RESULTS

The presented TL data is in significant disagreement with the few radiocarbon data on charcoal available from Ifri n'Ammar (Mikdad *et al.*, 2002). At Ifri n'Ammar a phenomena can be observed which is opposite to the 'normal' contamination, where more recent carbon is detected through the radiocarbon measurement of the soluble (humic acid) fraction from the charcoal. Here instead the soluble fraction produces ages older than the non-soluble fraction,

EVA-LUM	Palaeodose (Gy)	b-value (Gy μm²)	U (ppm)	Th (ppm)	K (ppm)	$\dot{D}_{int.eff}$ (μGy a⁻¹)	$\dot{D}_{\gamma\text{-ext.eff.}}$ (μGy a⁻¹)	$\dot{D}_{cosmic}$ (μGy a⁻¹)	$\dot{D}_{internal}$ (% $\dot{D}_{total}$)	Age (ka)
06/24	99.5 ± 2.7	2.41 ± 0.01	0.4 ± 0.04	0.13 ± 0.03	422 ± 14	113 ± 6	397	40	20	180.8 ± 31.1
07/13	869.8 ± 28.3	1.29 ± 0	12.5 ± 0.31	0.04 ± 0.01	272 ± 10	2,118 ± 46	399	40	83	339.7 ± 29.4*
06/25	113.9 ± 7.5	2.52 ± 0.01	0.78 ± 0.06	0.2 ± 0.03	1,660 ± 282	285 ± 24	397	40	39	157.5 ± 23.2
07/14	110.9 ± 15.1	1.21 ± 0	0.51 ± 0.07	0.04 ± 0.02	399 ± 16	117 ± 10	399	40	21	199.1 ± 35.5
06/26	153.1 ± 21.5	0.95 ± 0	2.14 ± 0.11	0.08 ± 0.05	477 ± 148	386 ± 19	399	40	47	185.2 ± 26
05/15	92.9 ± 6	0.03 ± 0	1.2 ± 0.09	0.07 ± 0.04	238 ± 10	196 ± 13	395	40	31	147.2 ± 23.6
06/28	129.3 ± 38.8	2.48 ± 0.03	0.69 ± 0.13	0.17 ± 0.03	1650 ± 46	265 ± 19	399	40	38	183.3 ± 30.4
								weighted average$		171 ± 12

Tab. 7. Layer 'Lower OI'. Results of TL measurements, Neutron Activation Analysis, dosimetry and ages. Uncertainties used in age calculation $\dot{D}_{\gamma\text{-ext.eff.}}$ and $\dot{D}_{cosmic}$ are 20 and 5 % respectively (see text). The external γ-dose rate was adjusted for 20 % increased moisture [* sample rejected by Dixon's outlier test; $ without rejected sample].

layer	humic acid	non soluble	CalPal 2007 Hulu	lab-#
Upper OS	51,330 +1,990/-1,590	39,700 +1,320/-1,130	43,620 ± 980	KIA-8822
Lower OS	57,390 +4,580/-2,900	38,740 +2,290/-1,780	42,850 ± 1,800	KIA-8823
Lower OS	>53,630	51,480 +1,470/-1,240	55,560 ± 2,520	KIA-8824
ibid.		51,370 +2,490/-1,900	54,960 ± 3,140	ibid.

Tab. 8. Radiocarbon results (Mikdad *et al.*, 2002) on the solulable and non-solulable fractions of charcoal samples, as well as calibrated non solulable radiocarbon data from the upper two Middle Paleolithic layers at Ifri n'Ammar.

which means that old and not young carbon was deposited in the charcoal. The source of this old carbon from older deposits is evidenced by the presence of thick deposits of caliche at Ifri n'Ammar, especially between layers XVII and XIX, XXII and XXIV and also between XXVI and XXXI. For the formation of caliche at the location of Ifri n'Ammar water needs to be percolating upwards through the sediments by evaporational processes, which indicates the presence of high temperatures together with considerable amounts of water. Such standing water was probably related to the water table of the nearby SW-NE wadi being much higher then today and the present day NW-SE running larger wadi not having been the main receiving water course.

The radiocarbon results on the non-solulable fraction thus suggest an age of about 40 ka for layer 'Upper OS' (with tanged items), and 40 – 50 ka for layer 'Lower OS' (Table 8). These results are at the fringes of the radiocarbon method and thus have to be questioned.

Charcoal is highly mobile in sediments and the samples were not retrieved from in situ and clearly visible hearths. Therefore the association of these samples with archaeological occupation of the layer they were found embedded in can be questioned. The complex geochemical history of the samples might also have induced changes in carbon composition of the sample, which are not recognizable and/or removable with the methods applied. In order to obtain ages close to the radiocarbon data, even when calibration is taken into account (Table 8), the external γ-dose rate had to have been higher by a factor of about 2.5 in the past. Such a difference or change in the external γ-dose rate is not possible without any indications of interruptions of the decay chains of radioactive isotopes in the sediment. A reduction of the moisture to 0 % (which is obviously an impossible scenario) is not sufficient to account for the observed age differences either and is in opposition to the general notion that the moisture in the site was higher at times.

Conclusions

The best age estimates for the layers at Ifri n'Ammar are provided by the weighted average TL-ages of 83 ± 6 ka for layer 'Upper OS' with its tanged pieces, 130 ± 8 ka for layer 'Lower OS' which lacks tanged items, 145 ± 9 ka for 'Upper OI', again containing tanged tools and the base of the sequence 'Lower OI' with 171 ± 12 ka where no tanged items were found. In fact, it could be argued that, especially for the two lower levels, the above age estimates are minimum ages, given the occurrence of thick packages of multiple caliches as strong indicators for the presence of a lot of water moving through the sediments, which would have attenuated the gamma radiation significantly. However, this parameter is hard to estimate and we therefore prefer to use a conservative approach by using the moisture content as it was measured today for the two upper levels, and make moderate conservative adjustments for the two lower levels.

The weighted TL data are in contrast to the age estimates provided by radiocarbon dating of charcoals originating from the upper two levels. They differ significantly and even when the older age estimates from the soluble fraction would be considered to reflect the 'true' age, there is no overlap at the 2σ level of probability. None of the parameters involved in calculating the TL ages can be modified within a plausible scenario to accommodate the radiocarbon ages results. Assuming that the charcoals are truly associated with the prehistoric events under question here, the radiocarbon data of the non-soluble fraction therefore has to be suspected of being contaminated by a small amount of modern carbon, which produced finite ages instead of infinite ones. On basis of the TL dating evidence the radiocarbon data is rejected.

The data presented above is given at a probability level of 65 % (1σ) only. But such a level is not sufficient for the interpretation and comparison of the data with other age estimates from other sites. The appropriate estimates of the heating of the flint artefacts from these layers are 71 – 95 ka for 'Upper OS', 114 – 146 ka for 'Lower OS', 127 – 163 ka for 'Upper OI' and 147 – 195 ka for 'Lower OI' at a probability of 95 % (2σ).

References

Adamiec, G./Aitken, M. J.
1998   Dose-rate conversion factors: update. Ancient TL 16, 37–50.

Aitken, M. J.
1985   Thermoluminescence dating. London, Academic Press.
1998   An Introduction to Optical Dating. The Dating of Quaternary Sediments by the Use of Photon-stimulated Luminescence. Oxford University Press, Oxford.

Alperson-Afil, N./Richter, D./Goren-Inbar, N.
2007   Phantom hearths and the use of fire at Gesher Benot Ya'Aqov, Israel. Paleoanthropology, 1–15.

Barbouti, A. I./Rastin, B. C.
1983   A study of the absolute intensity of muons at sea level and under various thickness absorber. Journal of Physics G, Nuclear Physics 9, 1577–1595.

Bellomo, R. V.
1993   A methodological approach for identifying archaeological evidence of fire resulting from human activities. Journal of Archaeological Science 20, 525–553.

Bøtter-Jensen, L./McKeever, S. W. S./Wintle, A. G.
2003   Optically Stimulated Luminescence Dosimetry. Amsterdam, Elsevier.

Bowman, S. G. E./Huntley, D. J.
1984   A new proposal for the expression of alpha efficiency in TL dating. Ancient TL 2, 6–8.

Guibert, P./Lahaye, C./Bechtel, F.
2009   The importance of U-series disequilibrium of sediments in luminescence dating: A case study at the Roc de Marsal Cave (Dordogne, France). Radiation Measurements 44, 223–231.

Mercier, N.
1991   Flint palaeodose determination at the onset of saturation. Nuclear Tracks and Radiation Measurements 18, 77–79.

Mikdad, A./Moser, J./Ben-Ncer, A.
2002   Recherche préhistoriques dans le gisement d'Ifri n'Ammar au Rif Oriental (Maroc). Premiers résultats. Beitr. Allg. u. Vgl. Arch. 22, 1–20.

Prescott, J. R./Stephan, L. G.
1982   The contribution of cosmic radiation to the environmental dose for TL dating. Latitude, altitude and depth dependancies. J. Council Europe PACT 6, 17–25.

Prescott, J. R./Hutton, J. T.
1994   Cosmic ray contributions to dose-rates for luminescence and ESR dating: large depths and long term variations. Radiation Measurements 23, 497–500.

Prescott, J. R./Huntley, D. J./Hutton, J. T.
1993   Estimation of equivalent dose in thermoluminescence dating – the 'Australian slide method'. Ancient TL 11, 1–5.

Richter, D.
2007   Advantages and limitations of thermoluminescence dating of heated flint from Paleolithic sites. Geoarchaeology 22, 671–683.

Richter, D./Krbetschek, M.
2006   A new Thermoluminescence dating technique for heated flint. Archaeometry 48, 695–705.

Richter, D./Waiblinger, J./Rink, W. J./Wagner, G. A.
2000   Thermoluminescence, Electron Spin Resonance and ^{14}C-Dating of the Late Middle and Early Upper Palaeolithic Site Geißenklösterle Cave in Southern Germany. Journal of Archaeological Science 27, 71–89.

Richter, D./Moser, J./Nami, M.
(in   New data from the site of Ifri n'Ammar
press)   (Morocco) and some remarks on the chronometric status of the Middle Paleolithic in NW-Africa. In: McPherron, S./Hublin, J.-J. (Hrsg.) Modern Origins: A North African Perspective. Vertebrate Paleobiology & Paleoanthropology. Springer – Heidelberg, New York.

Richter, D./Moser, J./Nami, M./Eiwanger, J./Mikdad, A. (submitted_a)
        New chronometric data from Ifri n'Ammar (Morocco) and the chronostratigraphical position of the 'Aterian' in the Maghreb. Journal of Human Evolution.

Richter, D./Zink, A./Guibert, P./Dombrowski, H./Neumaier, S. (submitted_b)
        Testing an environmental dosimetry system for in-situ sediment γ-dose measurements based on the OSL readout of α-Al$_2$O$_3$:C. (submitted to Radiation Protection Dosimetry).

Rorabacher, D. B.
1991   Statistical treatment for rejection of deviant values: critical values of Dixon's "Q" parameter and related subrange ratios at the 95 % confidence level. Analytical Chemistry 63, 139–146.

Sachs, L.
1992   Angewandte Statistik. Anwendung statistischer Methoden. 7th edition Berlin, Springer.

Sanzelle, S./Miallier, D./Pilleyre, T./Faïn, J./Montret, M.
1996   A new slide technique for regressing TL/ESR dose response curves – Intercomparison with other techniques. Radiation Measurements 26, 631–638.

Schwarcz, H. P.
1994   Current challenges to ESR dating. Quaternary Science Reviews 13, 601–605.

Tribolo, C./Mercier, N./Selo, M./Valladas, H./Joron, J. L./Reyss, J. L./Henshilwood, C./Sealy, J./Yates, R.
2006   TL dating of burnt lithics from Blombos Cave (South Africa): Further evidence fro the antiquity of modern human behaviour. Archaeometry 48, 341–357.

Valladas, G./Gillot, P. Y.
1978   Dating of the Olby lava flow using heated quartz pebbles: some problems. PACT, Revue du groupe européen d'études pour les techniques physiques, chimiques et mathématiques appliquées à l'archéologie 2, 141–150.

Wagner, G. A.

1998   Age Determination of Young Rocks and Artifacts. Berlin, Springer.

Wintle, A. G./Aitken, M. J.

1977   Thermoluminescence dating of burnt flint: application to a Lower Palaeolithic site, Terra Amata. Archaeometry 19, 111–130.

Dr. Daniel Richter
Department of Human Evolution
Max-Planck-Institute for Evolutionary Anthropology
Deutscher Platz 6
04103 Leipzig
Deutschland